Neuron
Article

Neuronal Activity Drives Localized Blood-Brain-Barrier Transport of Serum Insulin-like Growth Factor-I into the CNS

Takeshi Nishijima,[1,5] Joaquin Piriz,[1,5,6] Sylvie Duflot,[1,5] Ana M. Fernandez,[1] Gema Gaitan,[1] Ulises Gomez-Pinedo,[2] Jose M. Garcia Verdugo,[2] Felix Leroy,[1] Hideaki Soya,[3] Angel Nuñez,[4] and Ignacio Torres-Aleman[1,*]
[1]Cajal Institute, CSIC and CIBERNED, 28002 Madrid, Spain
[2]University of Valencia, CIPF, and CIBERNED, 46110 Valencia, Spain
[3]University of Tsukuba, Tsukuba 305-8574, Japan
[4]Autonoma University, 28029 Madrid, Spain
[5]These authors contributed equally to this work
[6]Present address: Laboratorio de Fisiologia y Biologia Molecular (LFBM-IFIBYNE), C1428EHA Buenos Aires, Argentina
*Correspondence: torres@cajal.csic.es
DOI 10.1016/j.neuron.2010.08.007

SUMMARY

Upon entry into the central nervous system (CNS), serum insulin-like growth factor-1 (IGF-I) modulates neuronal growth, survival, and excitability. Yet mechanisms that trigger IGF-I entry across the blood-brain barrier remain unclear. We show that neuronal activity elicited by electrical, sensory, or behavioral stimulation increases IGF-I input in activated regions. Entrance of serum IGF-I is triggered by diffusible messengers (i.e., ATP, arachidonic acid derivatives) released during neurovascular coupling. These messengers stimulate matrix metalloproteinase-9, leading to cleavage of the IGF binding protein-3 (IGFBP-3). Cleavage of IGFBP-3 allows the passage of serum IGF-I into the CNS through an interaction with the endothelial transporter lipoprotein related receptor 1. Activity-dependent entrance of serum IGF-I into the CNS may help to explain disparate observations such as proneurogenic effects of epilepsy, rehabilitatory effects of neural stimulation, and modulatory effects of blood flow on brain activity.

INTRODUCTION

The blood-brain barriers (BBB) located at brain vessels and choroid plexuses regulate passage of blood constituents into the brain parenchyma and cerebrospinal fluid (CSF), respectively (Abbott et al., 2010). Once considered an almost impermeable barrier for serum proteins, it is now apparent that many circulating hormones and growth factors can cross the BBB through specific transport mechanisms that usually involve their cognate receptors (Banks, 2006). However, the physiological significance of this blood-to-brain traffic of hormones and growth factors remains uncertain.

Insulin-like growth factor I (IGF-I), a peptide with ample neuroprotective activity (Russo et al., 2005), is one of the growth factors found to enter the brain from the circulation (Pardridge, 1993; Carro et al., 2000; Pulford and Ishii, 2001; Reinhardt and Bondy, 1994). Circulating IGF-I is produced mostly by the liver and is an important mediator of growth hormone actions in body growth and tissue remodeling. In addition, serum IGF-I shows a wide neuroactive profile that hints to an important role in brain homeostasis. Thus, blood-borne IGF-I modulates brain vessel growth (Lopez-Lopez et al., 2004), adult neurogenesis (Aberg et al., 2000), neuronal excitability (Nuñez et al., 2003), or even cognitive function (Trejo et al., 2007). Collectively, these observations provide a strong rationale for the need of circulating IGF-I to cross the BBB. Notably, the BBB architecture is well suited to transport serum IGF-I into the brain; both brain vessels and glial end-feet surrounding them express IGF-I receptors (García-Segura et al., 1991). If IGF-I is transferred by endothelial cells into the perivascular space, surrounding glial end-feet from astrocytes, able to endocytose IGF-I (Auletta et al., 1992), could transfer IGF-I to adjacent neurons through trans-endocytosis or a related process. Indeed, while upon binding to its membrane receptor IGF-I is internalized and mostly degraded (Geary et al., 1989), several cell types can translocate intact IGF-I to other cell compartments or even export it outside the cell (Zapf et al., 1994).

The choroid plexus epithelium at the blood-CSF interface also expresses high levels of IGF-I receptors (Marks et al., 1991). In previous work we found that increases in systemic IGF-I led to increased passage into the CSF through a mechanism involving the multicargo protein transporter low-density lipoprotein receptor related protein 2 (LRP2) located in this sealed epithelium (Carro et al., 2000, 2005). Therefore, a tonic transfer of serum IGF-I into the CSF may be explained by physiological oscillations in blood IGF-I levels (Carro et al., 2000). However, serum IGF-I levels usually remain very steady. Thus, a mechanism involving regulated passage of serum IGF-I may also coexist with this tonic input. A possible regulatory mechanism independent of changes in serum IGF-I levels may be activity driven.

Brain activity dictates transfer of oxygen and nutrients from the circulation into activated regions through a ''neurovascular coupling'' process described long ago (Roy and Sherrington, 1890). This process recruits all the cellular components of the neurovascular unit, with astrocytes serving an important intermediary role between neuronal activation and endothelial transport of oxygen and glucose (Zonta et al., 2003). Although the intracellular pathways involved in neurovascular coupling are not fully understood, a wealth of data indicate that diverse mediators released in response to neuronal glutamate (arachidonic acid derivatives, ATP, etc.) influence the microcirculation, allowing local increased passage of glucose and other nutrients through brain endothelial cells.

IGF-I in blood travels as a complex with an insulin-like binding protein 3 (IGFBP-3) and an ''acid labile subunit'' chaperone that regulates availability to target tissues by regulated release of IGF-I. Although the details of the trans-endothelial transport of IGF-I are not known, the tertiary complex probably tethers/associates to blood vessels to deliver IGF-I to endothelial cells after cleavage of IGFBP-3 by proteases. IGFBP-3 associates to the extracellular matrix and to membrane proteins such as LRP1. This membrane cargo-transporter mediates transcytosis of ligands across brain endothelial cells and has been postulated to be a cellular receptor for IGFBP-3 (Huang et al., 2003). LRP1 is abundantly expressed in brain endothelium and interacts with the insulin receptor (Bilodeau et al., 2009), which is closely related to the IGF-I receptor. Altogether, these characteristics make LRP-1 an attractive candidate to serve as a targeting platform for the circulating IGF-I/IGFBP-3 complex.

In the present work we explored whether brain activity modulates entrance of serum IGF-I and possible mechanisms involved. We observed that serum IGF-I input to the brain is regulated by an activity-driven process that includes changes in BBB permeability to serum IGF-I. This process is initiated by the release of glutamate at active regions. Thereafter, two parallel processes are set in motion: vasodilation to increase local availability of serum IGF-I and increased activity of matrix metalloprotease 9 (MMP9), an IGFBP3 protease already reported to be released in response to neuronal activity (Michaluk and Kaczmarek, 2007). The combined action of these two processes result in increased local availability of free serum IGF-I that is transcytosed through an LRP1-dependent mechanism.

RESULTS

Neuronal Activity Stimulates Uptake of Serum IGF-I

To assess mechanisms by which IGF-I might penetrate the BBB in response to neuronal activity, we used a combination of experimental approaches. First, we placed a stimulating electrode in the inferior cerebellar peduncle of rats receiving a bolus injection of human recombinant IGF-I (hIGF-I; 10 μg/100 g) in the carotid artery immediately before stimulation. By using a human-specific IGF-I ELISA, we distinguished between exogenous and endogenous (rat brain) IGF-I. As previously documented (Carro et al., 2000), hIGF-I was detected in different brain regions after systemic delivery. However, electrical stimulation (15 min, 5 Hz) of the cerebellar peduncle elicited an additional significant increase in cerebellar hIGF-I levels (Figure 1A). Nonstimulated regions such as the cerebral cortex did not show differences between stimulated and sham-stimulated animals (Figure 1A).

To assess whether systemic IGF-I accumulates in active brain areas regardless of region and type of stimulus, we activated the rat somatosensory cortex by unilateral whisker stimulation (60 min, 2 or 5 Hz). As seen in Figure 1B, stimulation of the vibrissae at 2 Hz effectively activated cortical somatosensory neurons, whereas at 5 Hz stimulation was dumped (Figure 1B, inset) because of neuronal desensitization (Chung et al., 2002). Accordingly, only stimulation of the whiskers at 2 Hz increased hIGF-I in somatosensory cortex as compared to animals stimulated at 5 Hz or sham-stimulated animals (Figure 1B). Frequency-dependent uptake of IGF-I by the brain correlates with frequency-dependent changes in cerebral blood flow in the barrel cortex during whisker stimulation (see below). These observations further confirmed that entrance of systemic IGF-I is regulated by neuronal activity. A region unrelated to the stimulation site such as the olfactory bulb, which had relatively high levels of hIGF-I after systemic injection, did not show stimulus-dependent increases in hIGF-I (not shown). Local IGF-I synthesis was not modified by stimulation; IGF-I mRNA levels in the stimulated somatosensory cortex did not differ from those in the unstimulated side (Figure S1A available online). Further, the IGF-I receptor was more activated in the stimulated than in the nonstimulated somatosensory cortex, as determined by increased levels of the Tyr-phosphorylated form of the receptor (Figure 1C). The latter confirms increased IGF-I input in the stimulated area.

We next assessed whether natural alterations in brain activity patterns, resulting from normal behavioral patterns, regulate IGF-I entry into the CNS. Mice submitted to a brief episode (2 hr) of environmental enrichment including multiple sensorimotor stimuli and increased social engagement, showed a 60% increase in hippocampal IGF-I levels compared to animals staying in their normal cages (Figure 1D). In addition, phosphorylation levels of hippocampal IGF-I receptor were significantly higher after environmental enrichment (Figure 1E). Thus, IGF-I input to this brain area appears augmented by environmental enrichment.

As systemic administration of IGF-I modulates basal neuronal excitability (Nuñez et al., 2003), we determined whether IGF-I also influences neuronal output in stimulated brain areas. Infusion of the IGF-I receptor antagonist PPP in the somatosensory cortex during unilateral tactile stimulation of the whiskers significantly reduced neuronal activation in this area. Under control conditions, whisker deflections (20 ms duration) induced spike firing in the primary somatosensory cortex of 2.9 spikes/stimulus (Figure 1F). However, intracortical application of PPP (2.5 μM) reduced cortical responses to 2.2 spikes/stimulus 15 min after application ($p = 0.005$) and to 1.9 spikes/stimulus 30 min later (Figure 1F, lower panel; $n = 19$ cells; $p = 0.004$). These results strongly suggest that IGF-I input into active brain regions has a functional impact.

Activity-Dependent Entrance of Serum IGF-I across Brain Vessels

Albeit at lower levels, nonstimulated brain areas also accumulate hIGF-I after intracarotid injection (i.e., cortex in Figure 1A).

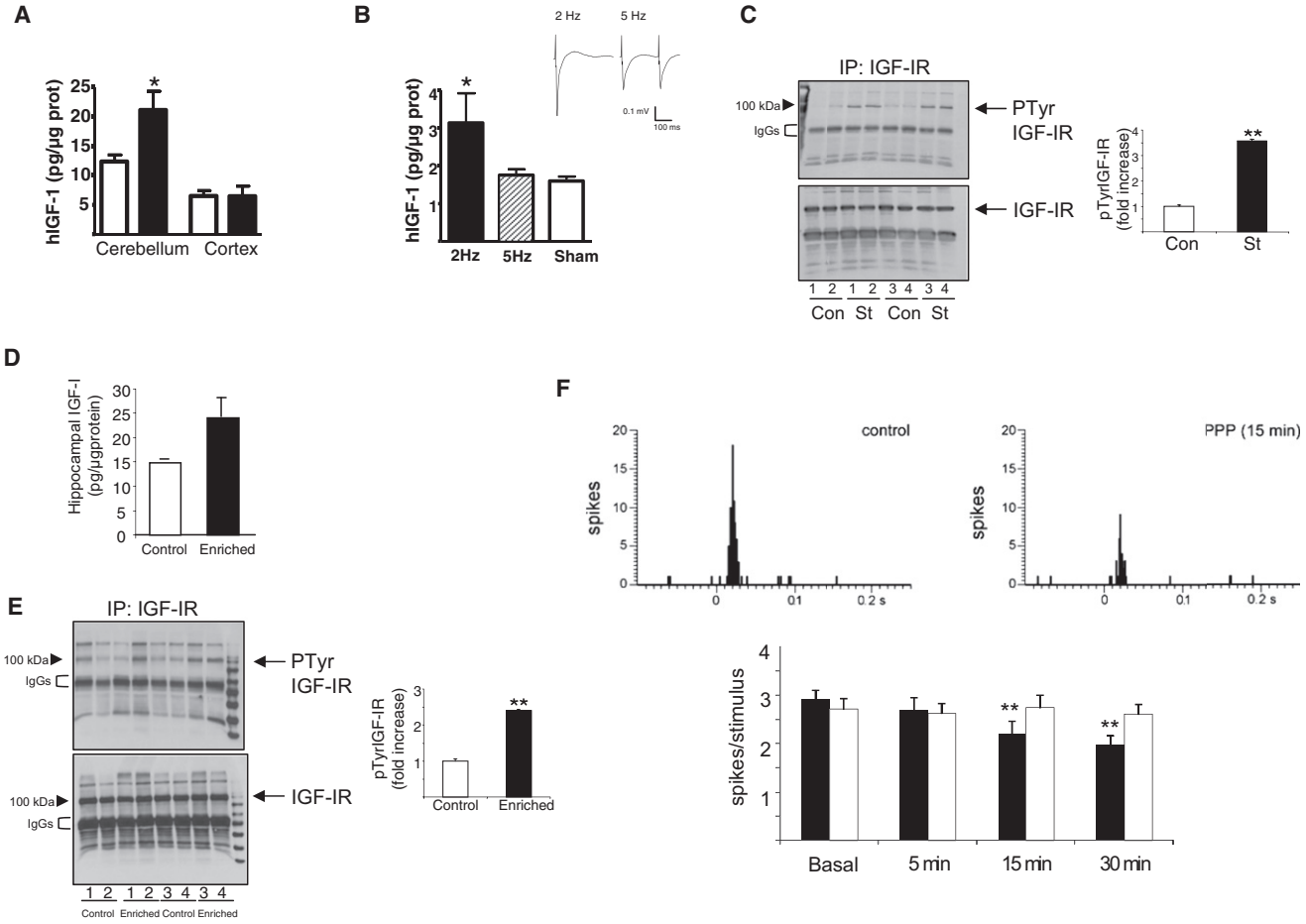

Figure 1. Active Brain Areas Accumulate Systemic IGF-I

(A) Electrical stimulation of the rat cerebellar peduncle (black bars) increased hIGF-I levels in cerebellum, as compared to sham-stimulated rats (white bars). Unstimulated areas such as the cerebral cortex did not show differences between stimulated and nonstimulated animals. Rats received hIGF-I through the carotid artery before stimulation of the inferior cerebellar peduncle (n = 7 per group; *p < 0.05).

(B) Electrical stimulation of the rat whiskers increased hIGF-I in the contralateral somatosensory cortex in a frequency-dependent fashion. Unilateral vibrissae stimulation at 2 Hz activates cortical somatosensory neurons, whereas at 5 Hz stimulation is dumped due to neuronal desensitization (inset shows averages of representative vibrissae deflection responses at somatosensory cortex; n = 10; *p < 0.05). Sham: nonstimulated animals.

(C) In 2 Hz-stimulated animals, levels of pTyr IGF-IR were significantly higher in the stimulated barrel cortex than in the ipsilateral, nonstimulated side (n = 10, **p < 0.01). Four representative animals (coded 1–4) are shown in blot. Quantitation histograms are shown after normalization with total IGF-IR levels (lower blot). Con, control, nonstimulated side; St, stimulated side; IgGs, band corresponding to the antibody used in immunoprecipitation.

(D) Hippocampal levels of IGF-I after 2 hr of enriched housing in mice (n = 19–20).

(E) Hippocampal levels of pTyrIGF-I receptor after environmental enrichment. Four representative animals for each group are shown. Levels of pTyr IGF-I receptor were normalized with total IGF-I receptor. Densitometric analysis of normalized western blots is shown (n = 10; Student's t test, **p < 0.001).

(F) Infusion of the IGF-I receptor antagonist PPP in the somatosensory cortex during unilateral tactile stimulation of the whiskers reduced neuronal activation in contralateral cortex. Upper: peristimulus time histograms of a representative S1 cortical neuron to whisker deflection (20 ms duration) in control (left) and after 15 min of PPP (right). Lower: mean tactile responses to whisker deflections in S1 cortical neurons. PPP (solid bars), but not the vehicle (empty bars), reduced tactile responses (n = 19; **p = 0.004).

Results are mean ± SEM (indicated by error bars) in this and subsequent figures. See also Figure S1.

Hence, we next determined whether systemic hIGF-I entered into the brain after neuronal activation through the blood-CSF interface (Carro et al., 2000). We assessed levels of hIGF-I in CSF after whisker stimulation and found no changes as compared to nonstimulated animals (Figure S1B). This suggested that activity-dependent entrance of systemic hIGF-I occurs through a different pathway. In agreement with this, when hIGF-I (5 µg/rat) was directly delivered into the CSF (Figure S1C), no stimulus-dependent increases of hIGF-I in the activated somatosensory cortex were seen (Figure S1D). This also indicated that cerebrospinal fluid IGF-I does not redistribute to active brain regions. Hence, the other possible route of entrance of circulating IGF-I into active brain areas is the local vasculature. Indeed, administration of digoxigenin-labeled

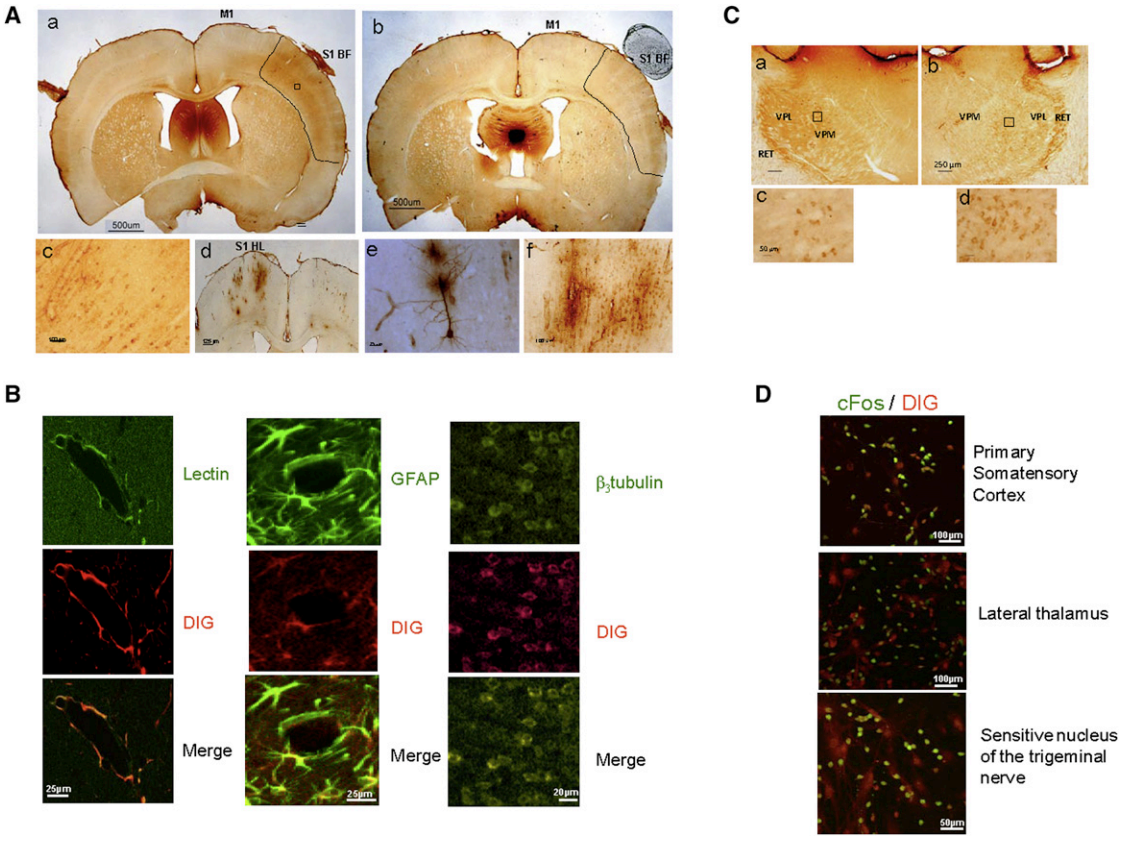

Figure 2. Neuronal Activation Triggers Entrance of Circulating IGF-I

(A) Panels a and b: Digoxigenin immunostaining in somatosensory cortex of whisker-stimulated rats receiving an intracarotid injection of digoxigenin-IGF-I prior to stimulation (a); not stimulated rats (b). Note the presence of immunostaining in the stimulated side of the cortex. Dashed area indicates somatosensory cortex. No staining is observed in nonstimulated animals. Panel c: Magnification of the square area in a (stimulated side). Neuronal-like profiles and vessels appear stained. M1, primary motor cortex; S1BF, primary sensory cortex barrel field area. Panel d: Digoxigenin immunostaining in rat primary sensitive cortex in the area corresponding to hind limbs (S1HL) after sciatic nerve stimulation. Panel e: Immunostaining with anti-digoxigenin shows a Dig-IGF-I accumulating neuron in the vicinity of an stained vessel in the somatosensory cortex after sciatic nerve stimulation. Panel f: Magnification of the same cortical area in a different animal after sciatic nerve stimulation. Dig-immunopositive neuron-like cells and vessels are seen. Representative animals are shown.

(B) After whisker stimulation, double immunocytochemistry with anti-digoxigenin and cell-specific markers denoted costaining of Dig-IGF-I in endothelial cells (tomato lectin$^+$), astrocytes (GFAP$^+$), and neurons ($\beta_3$tubulin$^+$) in the stimulated side. A small vessel in barrel cortex is shown. Astrocytes surrounding a large vessel are shown.

(C) Panels a and b: Digoxigenin immunostaining in the dorsal thalamus of nonstimulated (a) and stimulated (b) rats. Panels c and d: Magnification of the square areas in a and b. Note the increased number of stained neuron-like cells in the stimulated side. VPM, ventral postero-medial thalamus; VPL, ventral postero-lateral thalamus; RET, reticular nucleus of the thalamus.

(D) Stimulated brain areas along the whisker-barrrel cortex pathway accumulate Dig-IGF-I. Neuronal activation determined by c-*fos* staining (green) showed overlapping of Dig-IGF-I staining (red) with active regions within this sensory pathway. Relay areas such as the sensitive nucleus of the trigeminal nerve, the lateral thalamus, or the primary somatosensoty cortex are shown.

See also Figure S2.

IGF-I (Dig-IGF-I) immediately before stimulation of the whiskers or the sciatic nerve resulted in specific digoxigenin immunostaining in the stimulated side of the somatosensory cortex (Figure 2A). Double immunostaining with cell-specific markers showed that Dig-IGF-I staining colocalized with brain vessels (lectin$^+$ cells), astrocytes (GFAP$^+$), and neurons ($\beta_3$tubulin$^+$) (Figure 2B). Cells with neuronal morphology costained for digoxigenin and IGF-I, indicating that digoxigenin remained attached to IGF-I (Figure S2A). Nonstimulated animals did not show immunoreactivity in somatosensory cortex (Figure 2A, panel b). Further, Dig-IGF-I staining was also prominent in the posterio-medial thalamus (Figure 2C) contralateral to the stimulated whisker pad. Because this thalamic relay is within the whisker-cortex pathway, this suggests a spatial overlap between activated areas and IGF-I uptake. In this regard, neuronal activation determined by c-*fos* immunoreactivity showed overlapping of Dig-IGF-I staining with active brain regions within this sensory pathway such as the sensitive nucleus of the trigeminal nerve, the lateral thalamus, and the primary somatosensory cortex (Figure 2D). Electron microscopy analysis combined with immunogold labeling confirmed the presence of Dig-IGF-I in various cell compartments of brain vessels and neurons (Figure 3).

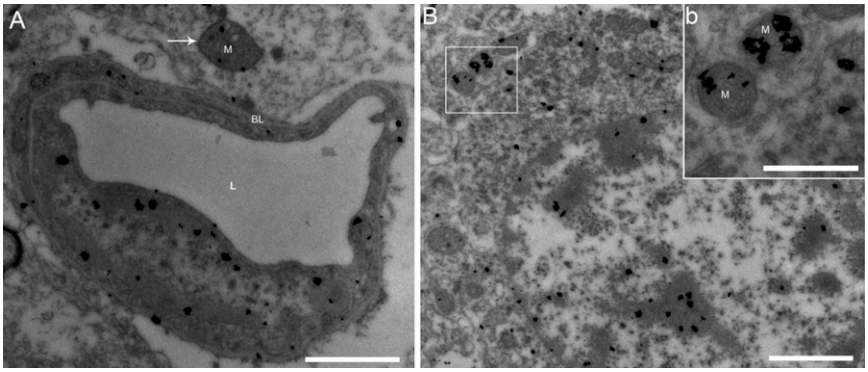

Figure 3. Systemically Injected Dig-IGF-I Localizes in Barrel Cortex Endothelial Cells and Neurons of Vibrissae-Stimulated Rats

(A) Electron microscopy photomicrograph of a brain endothelial cell showing immunogold staining against digoxigenin in cytoplasm, mitochondria, and chromatin. Arrow: stained mitochondria in an adjacent cell.

(B) Immunogold staining in the cell nucleus, mitochondria, and cytoplasm of a neuron. Inset: two labeled mitochondria are shown. M, mitochondria; L, lumen; BL, basal lamina.

Scale bars represent 1 μm in (A) and (B) and 500 nm in (b).

Staining was observed in the cell nucleus, mitochondria, and cytoplasm.

Neuro-trophic Coupling through Activity-Dependent Mediators

We next searched for mechanisms underlying activity-dependent entrance of systemic IGF-I through the brain vasculature. We focused on neuro-vascular coupling because it involves activity-dependent signaling from active synapses that modulate neighboring blood vessels to enhance local blood flow. As expected, unilateral electrical stimulation of the whisker pad enhanced regional cerebral blood flow (CBF) in the activated somatosensory cortex (Figure 4A). Increases in CBF were frequency dependent. Whereas stimulation at 2 Hz consistently raised it, at 5 Hz only a transient increase was observed (Figure S3A). This observation linked neuronal blood flow with IGF-I entrance because at 5 Hz no increases in hIGF-I entrance were appreciated (Figure 1B). Blood pressure, body temperature, and other systemic parameters (PCO_2, PO_2, etc.) remained stable during stimulation of the animals (Table 1). No changes were observed in CBF at the unstimulated barrel cortex (not shown). IGF-I may act as a vasodilator, so we determined whether intracarotid administration of IGF-I alters CBF in somatosensory cortex of nonstimulated animals and found no changes (Figure S3B).

Confirming the above observations, hIGF-I levels were significantly elevated in brain interstitial fluid collected through

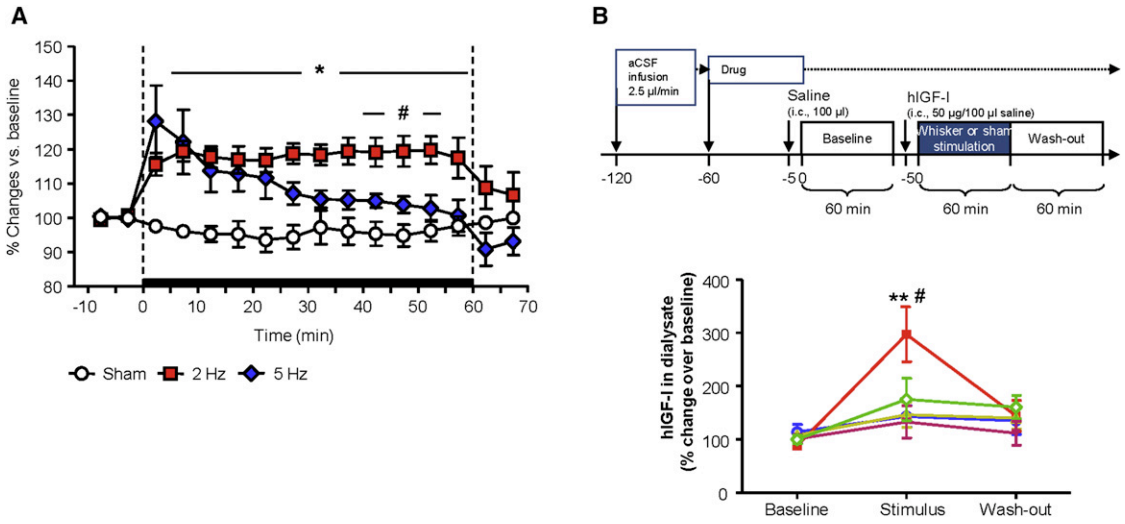

Figure 4. Activity-Dependent Entrance of Circulating IGF-I into the Brain

(A) Time course changes in CBF in barrel cortex during whisker stimulation. Data are averaged at 5 min intervals and represented as relative changes versus prestimulation values (−10–0 min). *p < 0.05 versus Sham; #p < 0.05 versus 5 Hz.

(B) hIGF-I in insterstitial fluid collected by microdyalisis from the somatosensory cortex was detectable only in whisker-stimulated animals. Experimental schedule employed in these experiments is shown in the upper panel.

Infusion of TTX to inhibit neuronal activity in the somatosensory cortex of vibrissae-stimulated animals abrogated the increase in hIGF-I levels. Infusion of L-NAME to inhibit vasodilation also blocked the stimulus-elicited increase in hIGF-I. Infusion of an MMP9 inhibitor also resulted in inhibition of the uptake of serum IGF-I. A two-way ANOVA revealed a significant interaction ($F(8,26) = 3.300$, $p < 0.01$) and a significant effect of time ($F(2, 26) = 11.80$, $p < 0.001$). A post-hoc Tukey's showed a significant difference between baseline and stimulation only in the stimulated group ($p < 0.01$). The stimulated group was also significantly different from sham-stimulated (#$p < 0.05$ by Student's t test). Blue open circle, sham (n = 6); red square, stimulated (n = 8); up triangle, stimulated+TTX (n = 5); down triangle, stimulated+L-NAME (n = 6); diamond, stimulated+MMP9 inhibitor (n = 6).

See also Figure S3.

Table 1. Changes in Arterial Blood Parameters and Body Temperature at Pre- and Poststimulations

	Pre		Post		
	Mean	SE	Mean	SE	
Control					
pH	7.43	0.01	7.43	0.01	n.s.
PCO_2 (mmHg)	36.0	1.4	38.2	0.6	n.s.
PO_2 (mmHg)	96.2	2.3	94.6	2.8	n.s.
Mean arteriyal pressure (mmHg)	98.5	3.8	100.1	4.4	n.s.
Heat rate (bpm)	371	6.1	375	6.5	n.s.
Body temperature (°C)	37.6	0.2	37.7	0.1	n.s.
2 Hz					
pH	7.44	0.00	7.43	0.01	n.s.
PCO_2 (mmHg)	36.3	2.5	38.0	2.4	n.s.
PO_2 (mmHg)	89.9	1.7	89.7	5.2	n.s.
Mean arteriyal pressure (mmHg)	93.2	5.9	98.5	3.0	n.s.
Heat rate (bpm)	349	5.2	358	6.1	n.s.
Body temperature (°C)	37.7	0.3	37.5	0.2	n.s.
5 Hz					
pH	7.44	0.01	7.42	0.01	n.s.
PCO_2 (mmHg)	38.3	1.0	38.1	0.9	n.s.
PO_2 (mmHg)	89.7	3.2	90.2	2.2	n.s.
Mean arteriyal pressure (mmHg)	90.4	4.1	91.4	4.8	n.s.
Heat rate (bpm)	382	18.8	391	13.2	n.s.
Body temperature (°C)	37.7	0.2	37.4	0.1	n.s.

n = 4–5. n.s., nonsignificant (paired t test).

a microdialysis probe placed in the somatosensory cortex of animals receiving vibrissae stimulation at 2 Hz ($p < 0.01$; Figure 4B). With this approach we determined the role of neuronal activity and vasodilation in activity-dependent IGF-I uptake. Intracortical infusion of TTX to inhibit neuronal activity (markedly reducing stimulus-induced increases in CBF, see Figure S3C) abrogated the increase in hIGF-I levels induced by vibrissae stimulation (Figure 4B). Similarly, infusion of the NO synthase inhibitor L-NAME to block vasodilation (which also results in diminished CBF after whisker stimulation, see Figure S3C) also abrogated this increase (Figure 4B). Collectively, these results indicate that both enhanced neuronal activity and increased blood flow are necessary for activity-dependent increases in serum IGF-I input to the brain.

Because passage of serum IGF-I through blood-brain-barrier cells may involve all the cells forming the neurovascular unit, we then used an in vitro system to determine whether the three main types of cells potentially involved in this purported blood-to-brain trafficking of IGF-I can internalize it. We found that endothelial cells, astrocytes, and neurons internalize intact biotinylated hIGF-I (bhIGF-I) after adding it to the culture medium (Figure 5A, upper blot). Elimination of nonspecific protein binding to the cell membrane prior to cell lysis by acid wash confirmed that the three types of cells internalize bhIGF-I (Figure 5A, lower blots). Further, as shown in Figure 5A, double immunostaining of biotin-labeled IGF-I and cell-specific markers show bhIGF-I immunoreactivity in endothelial cells (lectin$^+$ cells), astrocytes (GFAP$^+$), and neurons ($\beta_3$tubulin$^+$). We then hypothesized that once IGF-I binds to its receptors in endothelial cells, it will be internalized and translocated to adjacent glial end-feet surrounding brain vessels through a transcytosis process. To analyze this point we used a double chamber culture system with astrocytes as a feeder layer of endothelial cells in the upper chamber and neurons placed in the lower chamber to mimic the BBB architecture. Under these conditions, bhIGF-I was transported from the upper (i.e., apical side or "blood side" of the endothelial monolayer) to the lower (basolateral side or "brain side") chamber where neurons accumulated it (Figure 5B).

Next, we determined whether IGFBP-3 modulates internalization of IGF-I by endothelial cells. In the presence of IGFBP-3 (15 ng/ml), a weak but significant decrease in bhIGF-I endocytosis by brain endothelial cell cultures was observed (Figure 5C). The modest effect of exogenous IGFBP-3 could be due to the presence of endogenous IGFBP-3, because endothelial cells produce this binding protein (Lee et al., 1999). Indeed, IGFBP-3 was detected in the cultures (Figure 5D). To further substantiate a role of this binding protein in internalization of IGF-I by brain endothelial cells, we determined whether prostate-specific antigen (PSA), an IGFBP-3 protease, affected internalization of bhIGF-I. Addition of PSA greatly increased internalization of bhIGF-I by endothelial cells (Figure 5C). Because the effect was antagonized by IGFBP-3 (Figure 5C), this further supports its involvement. Further, endocytosis of bhIGF-I required the IGF-I receptor. Either transfection of human endothelioma cells with a dominant-negative IGF-I receptor (Figure 5E) or incubation of brain endothelial cells with the IGF-I receptor antagonist PPP blocked IGF-I internalization (Figure S4A).

Because PSA is a prostate protease unlikely to be produced by brain cells, we searched for alternative protease(s) involved in IGFBP-3 cleavage in brain endothelium. Among potential candidates we chose matrix metalloproteinase-9 (MMP9). MMP9 not only cleaves this binding protein (Figure 5F; Mañes et al., 1999) but is present in brain endothelium (Wang et al., 2006) and, most significantly, is modulated by brain activity (Michaluk and Kaczmarek, 2007). In the presence of active, but not inactive, MMP9 (50 ng/ml), brain endothelial cells endocytosed significantly more bhIGF-I. The effect was inhibited by IGFBP-3 ($p < 0.001$; Figure 5C). In contrast, another metalloprotease such as MMP8 did not increase IGF-I internalization by endothelial cells (Figure S4B). That another IGFBP-3 protease increased basal endocytosis confirmed that endothelial IGFBP-3 is interfering with bhIGF-I endocytosis in our cultures.

To gain further insight into the mechanism underlying transcytosis of IGF-I, we used the double chamber system mimicking the BBB, omitting neurons in the lower chamber to avoid IGF-I uptake. Under these conditions, bhIGF-I was transported from the upper (i.e., apical side or "blood side" of the endothelial monolayer) to the lower (basolateral side or "brain side") chamber, and its transport was significantly reduced when IGFBP-3 was added to the upper chamber

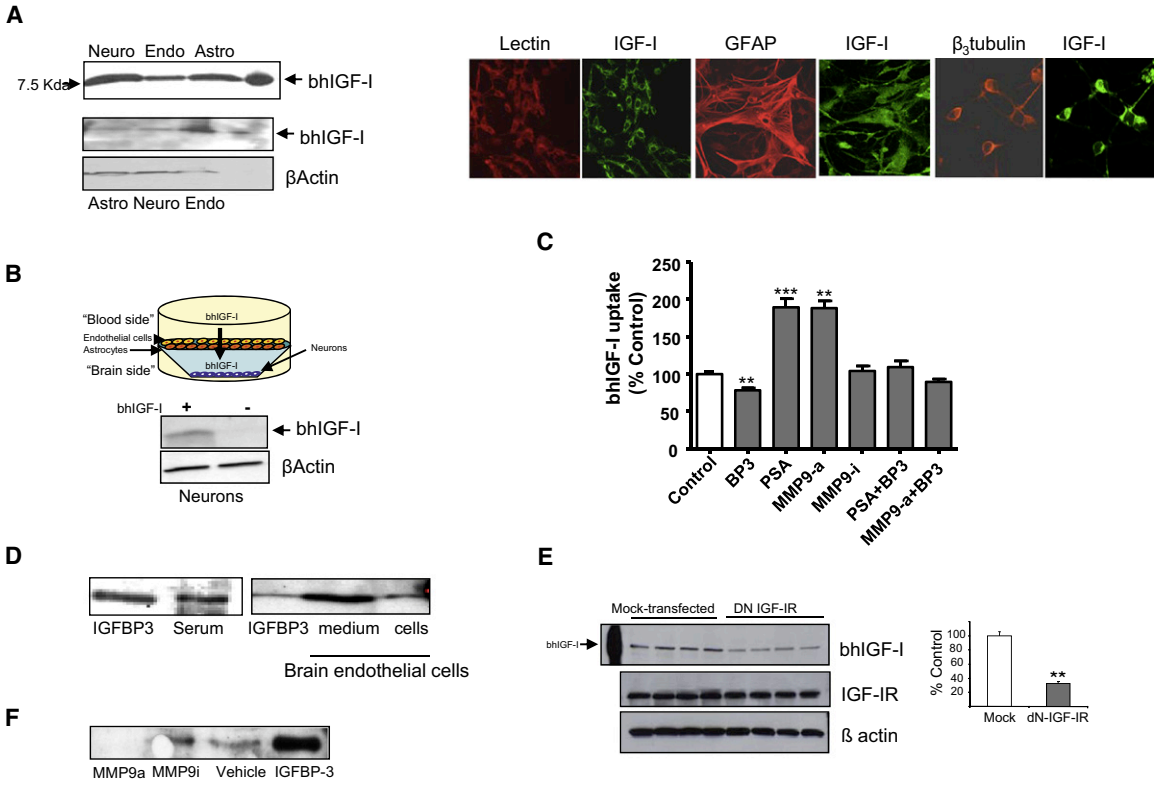

Figure 5. Mechanisms Involved in Transcytosis of IGF-I across the Blood-Brain Barrier

(A) Upper blot: Neurons (Neuro), brain endothelial cells (Endo), and astrocytes (Astro) accumulate bhIGF-I in vitro. Lower blots: After eliminating membrane bound bhIGF-I with acid wash prior to cell lysis, uptake of bhIGF-I by the three types of cells was still observed. Endothelial cells appear to take up more IGF-I than either neurons or astrocytes, as seen after normalization with β-actin. Synthetic bhIGF-I was loaded in the right lane. Micrographs: Double immunostaining with anti-bhIGF-I and GFAP (astrocytes), $\beta_3$tubulin (neurons), and tomato lectin (endothelium) showed intracellular IGF-I staining in the three types of cells.

(B) In a double-chamber well, endothelial/astrocyte cocultures in the upper chamber transport intact bhIGF-I to the lower chamber where neurons internalize it as evidenced by the presence of bhIGF-I in neuronal extracts. Scheme of experimental arrangement is shown.

(C) In the presence of active matrix metalloprotease 9 (MMP9a) but not inactive (MMP9i), significantly more bhIGF-I was endocytosed by endothelial cells. IGFBP-3 inhibited this effect. A similar effect was produced by PSA. $^{**}p < 0.01$ and $^{***}p < 0.001$ versus control; n = 5.

(D) IGFBP-3 is produced by endothelial cell cultures. IGFBP-3 and normal rat serum (NRS, that contains IGFBP-3) were run in parallel as controls.

(E) Human endothelioma cells transfected with a dominant-negative IGF-I receptor (DN-IGF-IR) endocytosed less bhIGF-I than mock-transfected cells. Representative blot of two experiments done in duplicate is shown. Quantitation histograms of internalized bhIGF-I shown in the right. Western blots of cell lysates for bIGF-I and IGF-IR/β-actin were run separately in different membranes ($^{**}p < 0.01$; n = 4).

(F) IGFBP-3 is cleaved by active (MMP9a) but not inactive MMP9 (MMP9i). Western blot of IGFBP-3 after treatment with MMP9 or the vehicle. Intact recombinant IGFBP-3 was run in the right lane.

See also Figure S4.

($p < 0.05$; Figure 6A). Confirming the effects seen in endothelial cell cultures, MMP9 also induced transcytosis of bhIGF-I through endothelial-astrocyte cocultures, an effect blocked by IGFBP-3 ($p < 0.01$; Figure 6A).

A key aspect of our proposal is that neuronal activation triggers serum IGF-I transcytosis from the blood into the brain. Glutamate released during neuronal activation signals to surrounding astrocytes (Haydon and Carmignoto, 2006; Perea et al., 2009) that in turn release vasoactive mediators (Iadecola and Nedergaard, 2007; Zonta et al., 2003). Accordingly, when glutamate (100 μM) was placed in the lower chamber (the brain side) of endothelial-astrocyte cocultures, IGF-I transcytosis from the upper (the blood side) to the lower chamber was greatly stimulated ($p < 0.01$; Figure 6B). The stimulatory action of glutamate was fully abolished by an MMP9 inhibitor, reinforcing a role for this protease in transcytosis of IGF-I (Figure 6B). Moreover, MMP9 was readily detected in endothelial cells (Figure 6C, upper blots) and glutamate stimulated it in endothelial-astrocyte cocultures (Figure 6C). In agreement with this, and as expected for a protease that is stimulated by brain activity (Michaluk and Kaczmarek, 2007), active MMP9 was increased in the stimulated somatosensory cortex (Figure 6D).

Next, we tested various vasoactive mediators proposed to be released in response to glutamate (Iadecola and Nedergaard, 2007). Among these, we chose those previously reported to enhance MMPs activity. The arachidonic acid derivatives prostaglandin E_2 (PGE_2) and 11,12 epoxyeicosatrienoic acid (EET), together with ATP, but not NO, increased bhIGF-I endocytosis by endothelial cells (Figure 7A). Another EET derivative, 8,9 EET, with lower vasodilatory activity (Harder et al., 1998) elicited

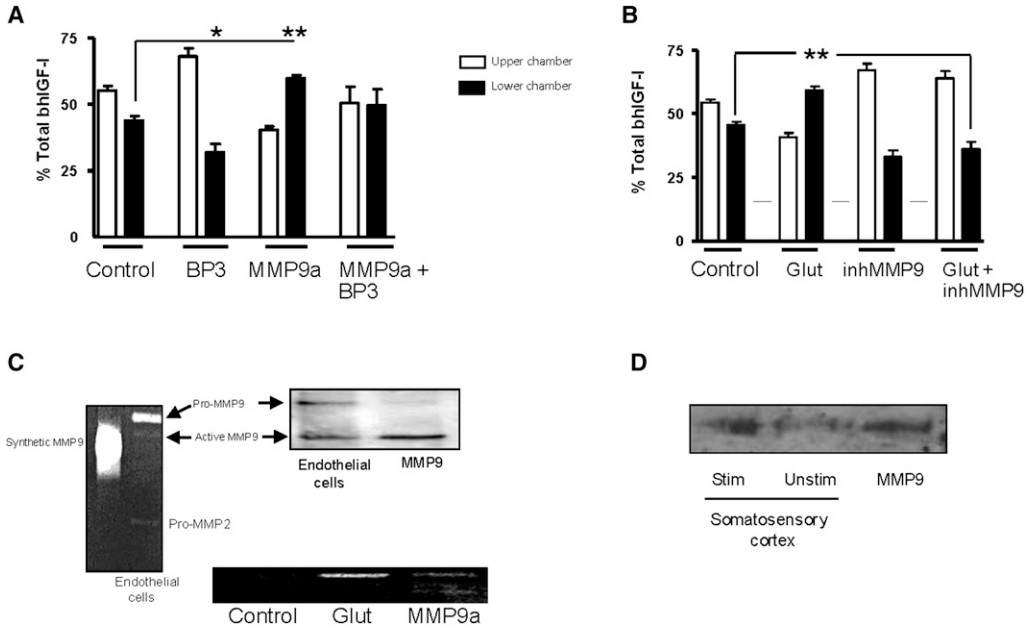

Figure 6. MMP9 Is Involved in Passage of Serum IGF-I across Brain Endothelium

(A) Passage of bhIGF-I through astrocytes/brain endothelial cells cocultures in double-chamber wells is modulated by IGFBP-3 and MMP9 in an opposite fashion. bhIGF-I and IGFBP-3 were placed in the "blood" side (upper chamber) whereas MMP9 was placed in the "brain" side (lower chamber) (n = 4; *p < 0.05 and **p < 0.01 versus lower chamber in controls).

(B) Transcytosis of bhIGF-I was stimulated by glutamate (100 μM), an effect inhibited with an MMP9 inhibitor (10 μM) (n = 7; **p < 0.01).

(C) MMP9 is present in endothelial cells (upper zymography and blot) and is stimulated by glutamate in endothelial-astrocyte cocultures (lower zymography). Representative experiments are shown (n = 2–3). Glut, glutamate; MMPa, active synthetic MMP9 was run as a control.

(D) Active MMP9 is increased in the stimulated somatosensory cortex. Western blot of MMP9 in stimulated (stim) and unstimulated (unstim) cortex of the same animal. Recombinant MMP9 was run in parallel.

a slightly smaller response: 70% ± 13% of that seen with 11,12 EET. Confirming these in vitro observations, infusion of a pharmacological dose of PGE_2 (5 mM) into the rat cerebral cortex (−0.5 mm from bregma, 1 mm depth), elicited widespread uptake of systemic digoxigenin-labeled IGF-I in the infused side (Figure 7B). Moreover, levels of PGE_2 in stimulated somatosensory cortex increased to 4.2 ± 0.01 pg/ml from 1.9 ± 0.01 pg/ml seen in sham-stimulated cortex ($p < 0.01$, n = 5 per group). Although these levels are well below the pharmacological doses used by us, they reinforce that local increases in PGE_2 participate in serum IGF-I transfer to the brain. We then determined whether these mediators require MMP-9 to increase IGF-I transcytosis. In the presence of an MMP9 inhibitor (inhMMP9), in vitro transcytosis of bhIGF-I by ATP, PGE_2, or EET was abrogated (Figure 7C). As in the case of PGE_2, this inhibition was not as complete as with the other mediators, and it is possible that PGE_2 recruits additional IGFBP-3 proteases.

Thereafter, we confirmed that MMP9 participates in activity-dependent uptake of serum IGF-I by the brain in vivo. Infusion of inhMMP9 into the somatosensory cortex of whisker-stimulated rats blocked the increase in brain interstitial fluid hIGF-I elicited by vibrissae stimulation (Figure 4B). Nonspecific hemodynamic responses of inhMMP9 were ruled out by infusing it into the somatosensory cortex and determining CBF responses to whisker stimulation (Figure S3C).

We next conducted an initial characterization of intracellular pathways involved in transfer of IGF-I in response to glutamate. We found that addition of a Ca^{2+} chelator (EGTA) to the culture medium inhibited the stimulatory action of glutamate on IGF-I transcytosis through astrocyte-endothelial cells cocultures, suggesting that the process is calcium dependent (Table 2). Coaddition of thapsigargin, an inhibitor of the ryanodine receptor that blocks intracellular Ca^{2+} stores, also resulted in abrogation of IGF-I transfer, further indicating the involvement of Ca^{2+} fluxes in this process (Table 2). Next, we tested various glutamate receptors antagonists and found that inhibition of ionotropic AMPA/Kainate receptors with CNQX or of mGluR5 with MPEP abrogated glutamate actions whereas NMDA and mGluR1 antagonists (AP5 and Lyly, respectively) did not alter the effect of glutamate (Table 2). Further, inhibition of prostanoid synthesis with the Cox inhibitor ibuprofen similarly blocked glutamate effects. Finally, no effect on glutamate actions was seen after inhibition of purinergic signaling via suramin (Table 2). Altogether, these results indicate that non-NMDA ionotropic and GluR5 metabotropic glutamate receptors are involved in transfer of IGF-I through astrocyte/endothelial cocultures and that prostanoid synthesis is required for this effect.

In response to neuronal activation, local levels of circulating IGF-I/IGFBP3 will increase as a result of increased local blood flow. We postulated that this complex would interact with LRP1/IGF-IR at endothelial cells for subsequent transcytosis of

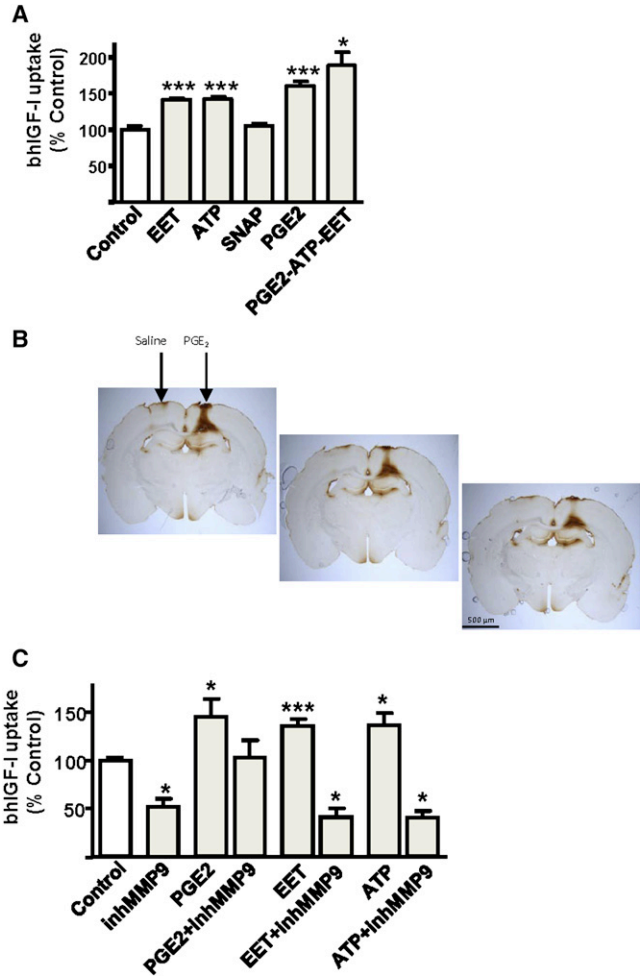

Figure 7. Mediators Involved in Neurovascular Coupling Modulate Passage of Blood-Borne IGF-I across Brain Endothelium

(A) Diffusible mediators released by astrocytes during neurovascular coupling stimulated endocytosis of bhIGF-I by brain endothelial cells. Prostaglandin E_2 (PGE_2), epoxyeicosatrienoic acid (EET), and ATP, but not NO (stimulated with SNAP), enhanced IGF-I internalization. Combined addition of the three compounds elicited a similar increase (n = 6–10).

(B) Infusion of PGE_2 into the cerebral cortex (−0.5 mm from bregma, 1 mm depth) of rats previously receiving an intracarotid injection of Dig-IGF-I results in robust digoxigenin staining in the infused side 30 min later. Note that both the contralateral, vehicle-infused side and the brain surface of the injected side showed low immunoreactivity attributable to local disruption of the BBB. Three consecutive 50 μm brain sections are shown.

(C) Enhanced internalization of bhIGF-I by PGE_2, EET, and ATP is inhibited by the MMP9 inhibitor. Note that the drug alone decreases bhIGF-I internalization to the same extent, indicating that endogenous MMP9 is required to internalize IGF-I (n = at least 3 experiments); ***p < 0.001, **p < 0.01, and *p < 0.05 versus control.

IGF-I. Confirming observations by others (Huang et al., 2003), we observed that LRP1 interacts with IGFBP3. LRP1 was coimmunoprecipitated with IGFBP3 in cell extracts from endothelial cultures treated with IGFBP3 (Figure 8A). LRP1 also coimmunoprecipitated with the IGF-I receptor in brain endothelial cells (Figure 8B). Conversely, an HA-tagged mini-LRP1 (lacking most of the extracellular domain of LRP1) expressed in brain endothelial cells coimmunoprecipitated with IGF-IR (Figure 8C). This suggested that the interaction between LRP1 and IGF-IR does not involve the extracellular ligand-binding domain of LRP1, leaving this domain free for binding of extracellular ligands such as IGFBP3. Finally, whereas endothelial cells expressing mini-LRP-1 internalized significantly more bhIGF-I than control cells (Figure 8D), HCMEC-D3 endothelioma cells expressing LRP1 siRNA internalized markedly less bhIGF-I than scramble siRNA-transfected cells (Figures 8E and 8F). Thus, interaction of LRP-1 with the IGF-I receptor and IGFBP-3 may target the IGF-I/IGFBP-3 complex to the IGF-I receptor and facilitate the subsequent transcytosis of IGF-I.

Table 2. Glutamate-Dependent Pathways Involved in Transcytosis of IGF-I across Endothelial-Astrocyte Cocultures in Double-Chamber Configuration

Treatment	IGF-I Transcytosis[a] (% Glutamate)	Statistical Significance[b]
Glutamate (n = 5)	100 ± 26	-[c]
Glutamate + AP5 (n = 5)	73 ± 31	0.24
Glutamate + CNQX (n = 5)	55 ± 11	0.001
Glutamate + lyly (n = 5)	184 ± 120	0.33
Glutamate + MPEP (n = 3)	0.3 ± 0.19	0.0004
Glutamate + thapsigargin (n = 3)	0.2 ± 0.5	0.0003
Glutamate + EGTA (n = 3)	5.1 ± 0.4	0.0006
Glutamate + ibuprofen (n = 3)	53 ± 21	0.002
Glutamate + suramin (n = 3)	113 ± 18	0.13

[a] Mean ± SEM

[b] As compared to glutamate (Student's t test).

[c] Glutamate induced a 217% ± 58% increase in IGF-I transcytosis over controls (p = 0.02).

DISCUSSION

The present results indicate that brain activity drives serum IGF-I input to activated areas. This novel link between neuronal activation and localized trophic support appears to recruit processes also involved in neurovascular coupling (Figure 8G). The fact that similar processes participate in allocating nutrient/oxygen supply and at the same time trophic support to active brain regions widens the physiological significance of activity-dependent processes in the brain. Importantly, these observations also provide a regulatory mechanism for the neuroactive actions of blood-borne IGF-I.

In line with these observations, the increases previously observed in the number of IGF-I immunoreactive neurons in the developing rat visual cortex after experience-dependent neuronal activity (Ciucci et al., 2007) or after environmental enrichment (Guzzetta et al., 2009) may be explained by localized transfer of serum IGF-I to the brain. Also, higher brain activity observed in human subjects with higher serum IGF-I levels (Arwert et al., 2005) agree with these findings. Together with recent evidence that neuronal activity increases antioxidant defenses in neurons (Léveillé et al., 2010; Papadia et al., 2008), these data provide further insight into the neuroprotective effects of neuronal activity.

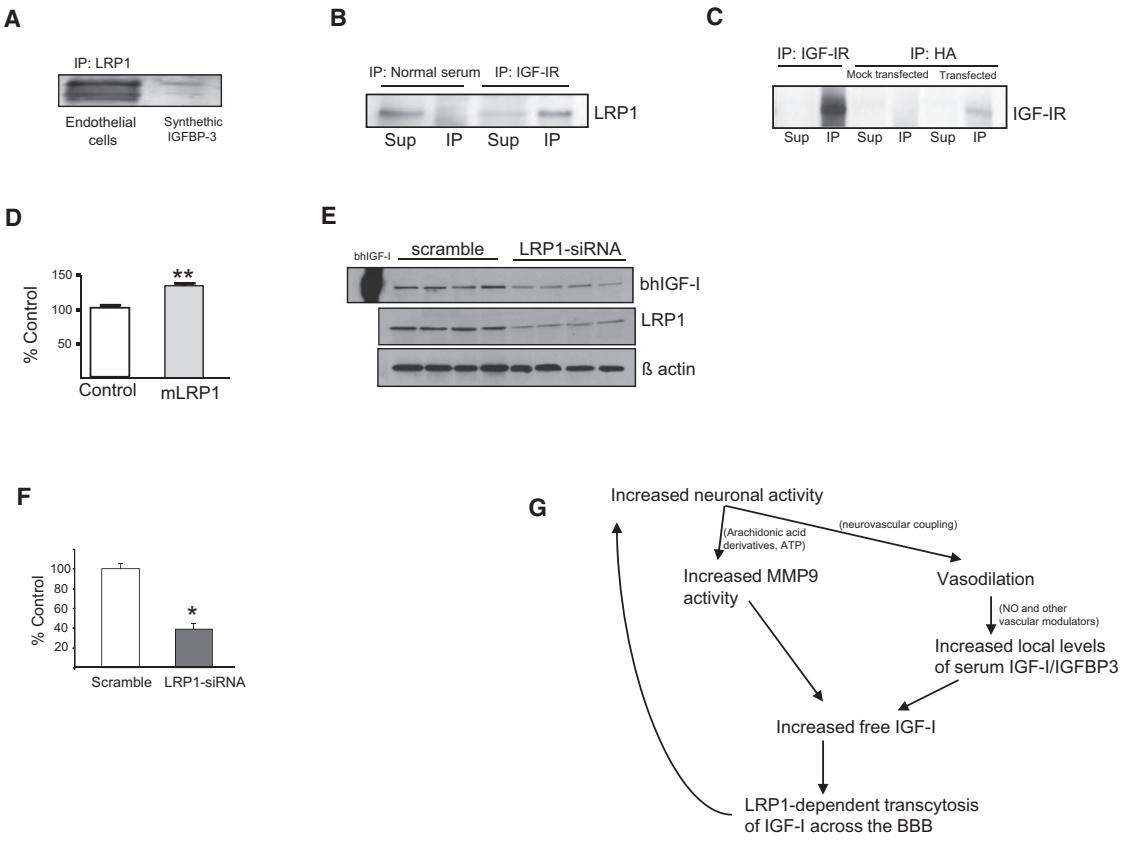

Figure 8. The IGF-I Receptor Interacts with LRP-1 in Brain Endothelial Cells

(A) LRP-1 coimmunoprecipitates with IGFBP-3. Standard IGFBP-3 is shown in the right lane.

(B) Coimmunoprecipitation of LRP1 and IGF-I receptors in brain endothelial cells. An LRP1 band was detected only in anti-IGF-I receptor (IGF-IR) immunoprecipitates (IP). Sup, supernatants.

(C) IGF-I receptors (IGF-IR) in brain endothelial cells coimmunoprecipitated with an HA-tagged mini-LRP1. Both supernatants (Sup) and immunoprecipitated pellets (IP) were assayed in an IGF-IR western blot. Controls included nontransfected cells and anti-IGF-IR immunoprecipitated fractions.

(D) Transfection of brain endothelial cells with mini-LRP1 enhanced endocytosis of bhIGF-I (**$p < 0.01$, $n = 4$).

(E and F) Transfection of the human endothelioma HCMEC-D3 with an LRP1 siRNA resulted in marked inhibition of bhIGF-I internalization. Control cultures were transfected with a scramble shRNA sequence.

(E) Western blots of cell lysates for bIGF-I and LRP1/β-actin were run separately in different membranes. Two experiments (in duplicate) were loaded/gel.

(F) Quantitation histograms (*$p < 0.05$; $n = 4$).

(G) Proposed mechanisms involved in serum IGF-I uptake by active brain regions. Increased neuronal activaty results in increased blood flow through neurovascular coupling. The resulting local vasodilation increases the amount of circulating IGF-I at the stimulated area. Neuronal activity also stimulates MMP9 activity that releases IGF-I from IGFBP3, allowing its internalization through the BBB in an LRP1-dependent process. Increased IGF-I input in stimulated areas stimulates neuronal activity. Through this step-wise pathway, serum IGF-I could modulate neuronal activity.

Transcytosis of molecules across the BBB is the most common way to modulate the permeability of this barrier (Banks, 2009). Neuronal activity modulates BBB permeability through neurovascular coupling. In turn, serum IGF-I participates in brain processes where neuronal activity is involved (synaptic plasticity, cognition, etc.). Therefore, we reasoned that neuronal activity could influence BBB permeability to serum IGF-I. Although activity-driven neurovascular and neuro-trophic coupling may share common upstream mechanisms such as vasodilation (Figure 8G), downstream mechanisms leading to increased glucose uptake and IGF-I transfer, respectively, probably diverge. In the former case neuronal release of glutamate leads to Ca^{2+} fluxes in astrocytes and subsequent release of diffusible mediators such as NO, arachidonic acid derivatives, ATP, etc., that modulate the microcirculation. Eventually, glucose and oxygen uptake are locally enhanced. Glucose uptake through the BBB is increased because glucose transporters are translocated to the cell membrane in response to a signaling mechanism that is still not well characterized. In neuro-trophic coupling, our initial observations suggest that together with vasodilation that will increase local availability of circulating IGF-I, glutamate release activates MMP9 in a process that appears to recruit several but not all of the mediators involved in vasogenic aspects of neurovascular coupling and that also involves Ca^{2+} mobilization. Thus, our initial in vitro pharmacological characterization suggests that IGF-I transfer depends on ionotropic (AMPA/kainate) and metabotropic (mGluR5) glutamate receptors, arachidonic acid derivatives,

and Ca^{2+} fluxes. However, more work is needed to ascertain the cellular and molecular pathways involved. In this regard, it should be noted that after many years of study, the mechanisms underlying neurovascular coupling are still under intense scrutiny (Shi et al., 2008).

At any rate, the present results allow us to propose an overview of the possible processes involved. Besides local changes in blood flow (in vivo inhibition of NO blocks IGF-I transfer), activation of MMP9 (and other proteases?) by diverse mediators (prostanoids, EETs, ATP) appears as the distinct characteristic required in IGF-I transfer across the BBB. MMP9 links neuronal activation with transfer of blood-borne IGF-I through an LRP1-dependent process. A similar process probably takes place at the choroid plexus, where the closely related receptor LRP2 also binds to the IGF-I receptor and actively participates in IGF-I transcytosis (Carro et al., 2005). Thus, two parallel processes, neurovascular coupling and neuro-trophic coupling, are set in motion by glutamate release at active synapses.

Several questions remain open. For instance, although the absence of changes in IGF-I mRNA synthesis after brain activation suggests that brain activity does not induce local IGF-I synthesis, locally activated IGF-I protein translation cannot be ruled out. This possibility would require further study. Further, although IGF-I immunoreactivity in the nucleus of astrocytes and neurons was already observed by us (García-Segura et al., 1991) and more recently confirmed in other cell types (Sehat et al., 2010), the role that IGF-I may play in these cellular organelles is still not fully understood.

Our observations also provide a mechanistic support for the cognitive reserve hypothesis of neuroprotection. Conceivably, neuro-trophic coupling may contribute to the beneficial effects of an active social life and higher education on brain function (Fratiglioni et al., 2004). Neuroprotective behaviors such as exercise or balanced diets also favor entrance of serum IGF-I into the brain (Carro et al., 2000; Dietrich et al., 2008), so this neuroprotective serum growth factor may be considered a common mediator of the beneficial effects of diverse lifestyle factors on brain health.

These findings may help explain disparate observations such as the proneurogenic effect of epilepsy or electroconvulsive therapy (Kempermann, 2002), the modulatory effect of blood flow on neuronal activity (Moore and Cao, 2008), or the rehabilitatory effect of neural stimulation (Kaelin-Lang, 2008). The latter may be of particular practical impact. The unifying thread in all these processes would be increased input of serum IGF-I to stimulated brain regions. In the first case, enhanced neurogenesis after neuronal hyperactivity could be explained by the potent neurogenic effects documented for serum IGF-I (Trejo et al., 2008). In the second case, activity-dependent entrance of serum IGF-I coupled to enhanced blood flow would conform to the "hemo-neural" hypothesis that proposes that diffusible blood-borne messengers modulate neuronal activity (Moore and Cao, 2008). Indeed, systemic IGF-I increases neuronal excitability (Nuñez et al., 2003) and levels of serum IGF-I correlate with brain vascular activation (Arwert et al., 2005). Finally, neural stimulation inducing the entrance of systemic IGF-I will in turn produce wide beneficial effects on activated areas through the ample neuroprotective actions of IGF-I (Carro et al., 2003). An unexplored aspect of these observations is the angiogenic role of serum IGF-I (Lopez-Lopez et al., 2004). As vessel formation is regulated by tissue demand, activity-dependent uptake of serum IGF-I through brain vessels would also impinge on vessels themselves. Altogether, activity-dependent entrance of a serum neuroprotective factor supports the use of neuro-rehabilitation procedures based on targeted neuronal stimulation of damaged areas.

EXPERIMENTAL PROCEDURES

In Vivo Procedures

Human recombinant IGF-I was administered in the carotid artery or into the brain lateral ventricle to adult male Wistar rats prior to the stimulation protocols. Drugs were directly infused into the primary somatosensory cortex. At the end of each experiment, brains were perfused with saline and processed for immunocytochemistry or frozen for various biochemical determinations. For barrel cortex sampling, the brain was cut rostro-caudally until the medial fusion of the anterior commisure (−0.3 mm from bregma). Thereafter, a 2 mm slice was made and a piece of the barrel cortex isolated through two incisions perpendicular to the surface of the cortex at 4.5 and 7 mm from midline. CSF was collected from the cisterna magna.

Stimulation Protocols

The rat inferior cerebellar peduncle was stimulated with 0.1 ms square pulses (50–100 μA) at 5 Hz frequency. The whisker pad was stimulated with a 1 ms square pulse (50–100 μA) with two subcutaneous electrodes located at the dorso-anterior and caudo-posterior edges of the whisker pad. Stimulus-evoked potentials were recorded in barrel cortex in some animals. Rat whiskers were also stimulated by an electronically gated air jet in 20 ms, 0.5 Hz pulses. The sciatic nerve was stimulated by delivering pulses of 100 μs, 0.5 Hz, and 10–50 μA. For sham stimulation, electrodes were placed without delivering any current. Behavioral stimulation of adult C57BL6J male mice consisted of enriched housing in a large arena with toys, exercise wheels, and 10 animals per cage.

Brain Microdialysis

A guide cannula was fixed above the barrel cortex contralateral to the stimulated whisker pad of adult rats, and after rats recovered from surgery, a microdialysis probe was inserted through it into the barrel cortex. The probe was infused with artificial cerebrospinal fluid in a push-pull manner. Infusion protocols are summarized in Figure 4B. Dialysates were collected at 60 min intervals to determine hIGF-I levels. Cannula placement was always confirmed by histology.

Cell Cultures and In Vitro Assays

All cultures were performed as described previously (Fernandez et al., 2007). Coculture of endothelial cells and astrocytes to mimic BBB architecture was performed as described by others with a double-chamber culture well (Perrière et al., 2007). Formation of a sealed monolayer was confirmed by measuring electrical resistance and retention of fluorescent dextran. In transcytosis and internalization assays, we used biotinylated IGF-I to distinguish it from endogenously produced IGF-I. Cells were transfected with siRNAs, mini-LRP1, or dominant-negative IGF-I receptor and used 48–72 hr later.

Cerebral Blood Flow Measurement

Cerebral blood flow was monitored during whisker pad stimulation with laser-Doppler flowmetry after performing a small craniotomy over the barrel cortex. The time constant was 0.01 s. Before and after stimulation, arterial blood gases and pressure were monitored. Data were averaged at 5 or 20 min intervals and represented as relative changes versus baseline.

In Vivo Recordings

After drilling a small hole in the skull over the SI cortex, unit recordings were recorded below the brain surface via tungsten microelectrodes. Unit

firing was filtered, amplified, and fed into a computer for offline analysis. Cortical field potentials were recorded at SI cortex, with tungsten macroelectrodes. Averages of the field potentials and summed peristimulus time histograms were calculated from 20 stimuli. Data were compared with Student's paired t test.

Immunoassays

Immunocytochemical assays were performed as previously described. First antibodies were omitted in control sections and no staining was observed (not shown). Human and murine IGF-I levels were determined by species-specific ELISAs as described (Trejo et al., 2007). A commercial ELISA was used to measure PGE2 in cortical lysates.

Gel Zymography

MMP-9 activity in glutamate-treated cultures and brain samples was assessed by gelatin zymography. Lysates were loaded under no reducing conditions onto 10% polyacrylamide-1% gelatin gels. To reveal the gelatinolytic activity, gels were stained with 0.25% brilliant blue and destained with 10% methanol and 7% acetic acid.

Pre-Embedding Immunogold Labeling and EM

Brain were perfused with 0.5% glutaraldehyde/2.5% paraformaldehyde and sections (50 μm) were immunostained with digoxigenin antibodies and a secondary antibody conjugated to colloidal gold, enhanced with silver, washed, postfixed with 2.5% glutaraldehyde for 20 min, washed, and postfixed with 1% osmium tetroxide. Immunostained sections were dehydrated and embedded in resin. Sixty nanometer sections were cut and collected on Formvar-coated single-slot grids, stained with uranyl acetate and lead citrate, and examined with a FEI Tecnai Spirit electron microscope.

Quantitative PCR

IGF-I qPCR was performed as described. Equivalent amounts of isolated total brain RNA served as template to synthesize cDNA. TaqMan probes and primers for IGF-I and for the control housekeeping gene, rRNA 18s, were used. IGF-I mRNA was normalized to the endogenous reference and expressed relative to the calibrator.

Statistics

One- and two-way ANOVAs were used for overall comparisons as indicated in the legends of the figures. Post-hoc tests included Tukey and Student's t test.

SUPPLEMENTAL INFORMATION

Supplemental Information includes Supplemental Experimental Procedures and four figures and can be found with this article online at doi:10.1016/j.neuron.2010.08.007.

ACKNOWLEDGMENTS

We are thankful to I. Alvarez, M. Garcia, M. Oliva, and L. Guinea for technical support and L. Genis and A. Trueba for help with the cell cultures. This work was funded by Spanish Ministry of Science (SAF2007-60051), by CIBERNED, and by a joint Japan-Spain collaborative program (JSPS-CSIC-2006JP0010). I.T.-A. is founder of a company (9% ownership) devoted to the use of IGF-I for neurodegenerative diseases.

Accepted: August 2, 2010
Published: September 8, 2010

REFERENCES

Abbott, N.J., Patabendige, A.A.K., Dolman, D.E.M., Yusof, S.R., and Begley, D.J. (2010). Structure and function of the blood-brain barrier. Neurobiol. Dis. *37*, 13–25.

Aberg, M.A., Aberg, N.D., Hedbäcker, H., Oscarsson, J., and Eriksson, P.S. (2000). Peripheral infusion of IGF-I selectively induces neurogenesis in the adult rat hippocampus. J. Neurosci. *20*, 2896–2903.

Arwert, L.I., Veltman, D.J., Deijen, J.B., Lammertsma, A.A., Jonker, C., and Drent, M.L. (2005). Memory performance and the growth hormone/insulin-like growth factor axis in elderly: a positron emission tomography study. Neuroendocrinology *81*, 31–40.

Auletta, M., Nielsen, F.C., and Gammeltoft, S. (1992). Receptor-mediated endocytosis and degradation of insulin-like growth factor I and II in neonatal rat astrocytes. J. Neurosci. Res. *31*, 14–20.

Banks, W.A. (2006). Denial versus dualism: the blood-brain barrier as an interface of the gut-brain axis. Endocrinology *147*, 2609–2610.

Banks, W.A. (2009). Mouse models of neurological disorders: A view from the blood-brain barrier. Biochim. Biophys. Acta, in press. Published online October 29, 2009. 10.1016/j.bbadis.2009.10.011.

Bilodeau, N., Fiset, A., Boulanger, M.C., Bhardwaj, S., Winstall, E., Lavoie, J.N., and Faure, R.L. (2009). Proteomic analysis of Src family kinases signaling complexes in golgi/endosomal fractions using a site-selective anti-phosphotyrosine antibody: Identification of LRP1-insulin receptor complexes. J. Proteome Res. *9*, 708–717.

Carro, E., Nuñez, A., Busiguina, S., and Torres-Aleman, I. (2000). Circulating insulin-like growth factor I mediates effects of exercise on the brain. J. Neurosci. *20*, 2926–2933.

Carro, E., Trejo, J.L., Núñez, A., and Torres-Aleman, I. (2003). Brain repair and neuroprotection by serum insulin-like growth factor I. Mol. Neurobiol. *27*, 153–162.

Carro, E., Spuch, C., Trejo, J.L., Antequera, D., and Torres-Aleman, I. (2005). Choroid plexus megalin is involved in neuroprotection by serum insulin-like growth factor I. J. Neurosci. *25*, 10884–10893.

Chung, S., Li, X., and Nelson, S.B. (2002). Short-term depression at thalamocortical synapses contributes to rapid adaptation of cortical sensory responses in vivo. Neuron *34*, 437–446.

Ciucci, F., Putignano, E., Baroncelli, L., Landi, S., Berardi, N., and Maffei, L. (2007). Insulin-like growth factor 1 (IGF-1) mediates the effects of enriched environment (EE) on visual cortical development. PLoS ONE *2*, e475.

Dietrich, M.O., Spuch, C., Antequera, D., Rodal, I., de Yébenes, J.G., Molina, J.A., Bermejo, F., and Carro, E. (2008). Megalin mediates the transport of leptin across the blood-CSF barrier. Neurobiol. Aging *29*, 902–912.

Fernandez, A.M., Fernandez, S., Carrero, P., Garcia-Garcia, M., and Torres-Aleman, I. (2007). Calcineurin in reactive astrocytes plays a key role in the interplay between proinflammatory and anti-inflammatory signals. J. Neurosci. *27*, 8745–8756.

Fratiglioni, L., Paillard-Borg, S., and Winblad, B. (2004). An active and socially integrated lifestyle in late life might protect against dementia. Lancet Neurol. *3*, 343–353.

García-Segura, L.M., Pérez, J., Pons, S., Rejas, M.T., and Torres-Alemán, I. (1991). Localization of insulin-like growth factor I (IGF-I)-like immunoreactivity in the developing and adult rat brain. Brain Res. *560*, 167–174.

Geary, E.S., Rosenfeld, R.G., and Hoffman, A.R. (1989). Insulin-like growth factor-I is internalized after binding to the type I insulin-like growth factor receptor. Horm. Metab. Res. *21*, 1–3.

Guzzetta, A., Baldini, S., Bancale, A., Baroncelli, L., Ciucci, F., Ghirri, P., Putignano, E., Sale, A., Viegi, A., Berardi, N., et al. (2009). Massage accelerates brain development and the maturation of visual function. J. Neurosci. *29*, 6042–6051.

Harder, D.R., Alkayed, N.J., Lange, A.R., Gebremedhin, D., and Roman, R.J. (1998). Functional hyperemia in the brain: hypothesis for astrocyte-derived vasodilator metabolites. Stroke *29*, 229–234.

Haydon, P.G., and Carmignoto, G. (2006). Astrocyte control of synaptic transmission and neurovascular coupling. Physiol. Rev. *86*, 1009–1031.

Huang, S.S., Ling, T.Y., Tseng, W.F., Huang, Y.H., Tang, F.M., Leal, S.M., and Huang, J.S. (2003). Cellular growth inhibition by IGFBP-3 and TGF-beta1 requires LRP-1. FASEB J. *17*, 2068–2081.

Iadecola, C., and Nedergaard, M. (2007). Glial regulation of the cerebral microvasculature. Nat. Neurosci. *10*, 1369–1376.

Kaelin-Lang, A. (2008). Enhancing rehabilitation of motor deficits with peripheral nerve stimulation. NeuroRehabilitation *23*, 89–93.

Kempermann, G. (2002). Regulation of adult hippocampal neurogenesis - implications for novel theories of major depression. Bipolar Disord. *4*, 17–33.

Lee, W.H., Wang, G.M., Yang, X.L., Seaman, L.B., and Vannucci, S.I. (1999). Perinatal hypoxia-ischemia decreased neuronal but increased cerebral vascular endothelial IGFBP3 expression. Endocrine *11*, 181–188.

Léveillé, F., Papadia, S., Fricker, M., Bell, K.F.S., Soriano, F.X., Martel, M.A., Puddifoot, C., Habel, M., Wyllie, D.J., Ikonomidou, C., et al. (2010). Suppression of the intrinsic apoptosis pathway by synaptic activity. J. Neurosci. *30*, 2623–2635.

Lopez-Lopez, C., LeRoith, D., and Torres-Aleman, I. (2004). Insulin-like growth factor I is required for vessel remodeling in the adult brain. Proc. Natl. Acad. Sci. USA *101*, 9833–9838.

Mañes, S., Llorente, M., Lacalle, R.A., Gómez-Moutón, C., Kremer, L., Mira, E., and Martínez-A, C. (1999). The matrix metalloproteinase-9 regulates the insulin-like growth factor-triggered autocrine response in DU-145 carcinoma cells. J. Biol. Chem. *274*, 6935–6945.

Marks, J.L., Porte, D., Jr., and Baskin, D.G. (1991). Localization of type I insulin-like growth factor receptor messenger RNA in the adult rat brain by in situ hybridization. Mol. Endocrinol. *5*, 1158–1168.

Michaluk, P., and Kaczmarek, L. (2007). Matrix metalloproteinase-9 in glutamate-dependent adult brain function and dysfunction. Cell Death Differ. *14*, 1255–1258.

Moore, C.I., and Cao, R. (2008). The hemo-neural hypothesis: on the role of blood flow in information processing. J. Neurophysiol. *99*, 2035–2047.

Nuñez, A., Carro, E., and Torres-Aleman, I. (2003). Insulin-like growth factor I modifies electrophysiological properties of rat brain stem neurons. J. Neurophysiol. *89*, 3008–3017.

Papadia, S., Soriano, F.X., Léveillé, F., Martel, M.A., Dakin, K.A., Hansen, H.H., Kaindl, A., Sifringer, M., Fowler, J., Stefovska, V., et al. (2008). Synaptic NMDA receptor activity boosts intrinsic antioxidant defenses. Nat. Neurosci. *11*, 476–487.

Pardridge, W.M. (1993). Transport of insulin-related peptides and glucose across the blood-brain barrier. Ann. N Y Acad. Sci. *692*, 126–137.

Perea, G., Navarrete, M., and Araque, A. (2009). Tripartite synapses: astrocytes process and control synaptic information. Trends Neurosci. *32*, 421–431.

Perrière, N., Yousif, S., Cazaubon, S., Chaverot, N., Bourasset, F., Cisternino, S., Declèves, X., Hori, S., Terasaki, T., Deli, M., et al. (2007). A functional in vitro model of rat blood-brain barrier for molecular analysis of efflux transporters. Brain Res. *1150*, 1–13.

Pulford, B.E., and Ishii, D.N. (2001). Uptake of circulating insulin-like growth factors (IGFs) into cerebrospinal fluid appears to be independent of the IGF receptors as well as IGF-binding proteins. Endocrinology *142*, 213–220.

Reinhardt, R.R., and Bondy, C.A. (1994). Insulin-like growth factors cross the blood-brain barrier. Endocrinology *135*, 1753–1761.

Roy, C.S., and Sherrington, C.S. (1890). On the regulation of the blood-supply of the brain. J. Physiol. *11*, 85–158, 17.

Russo, V.C., Gluckman, P.D., Feldman, E.L., and Werther, G.A. (2005). The insulin-like growth factor system and its pleiotropic functions in brain. Endocr. Rev. *26*, 916–943.

Sehat, B., Tofigh, A., Lin, Y., Trocmé, E., Liljedahl, U., Lagergren, J., and Larsson, O. (2010). SUMOylation mediates the nuclear translocation and signaling of the IGF-1 receptor. Sci. Signal. *3*, ra10.

Shi, Y., Liu, X., Gebremedhin, D., Falck, J.R., Harder, D.R., and Koehler, R.C. (2008). Interaction of mechanisms involving epoxyeicosatrienoic acids, adenosine receptors, and metabotropic glutamate receptors in neurovascular coupling in rat whisker barrel cortex. J. Cereb. Blood Flow Metab. *28*, 111–125.

Trejo, J.L., Piriz, J., Llorens-Martin, M.V., Fernandez, A.M., Bolós, M., LeRoith, D., Nuñez, A., and Torres-Aleman, I. (2007). Central actions of liver-derived insulin-like growth factor I underlying its pro-cognitive effects. Mol. Psychiatry *12*, 1118–1128.

Trejo, J.L., Llorens-Martín, M.V., and Torres-Alemán, I. (2008). The effects of exercise on spatial learning and anxiety-like behavior are mediated by an IGF-I-dependent mechanism related to hippocampal neurogenesis. Mol. Cell. Neurosci. *37*, 402–411.

Wang, L., Zhang, Z.G., Zhang, R.L., Gregg, S.R., Hozeska-Solgot, A., LeTourneau, Y., Wang, Y., and Chopp, M. (2006). Matrix metalloproteinase 2 (MMP2) and MMP9 secreted by erythropoietin-activated endothelial cells promote neural progenitor cell migration. J. Neurosci. *26*, 5996–6003.

Zapf, A., Hsu, D., and Olefsky, J.M. (1994). Comparison of the intracellular itineraries of insulin-like growth factor-I and insulin and their receptors in Rat-1 fibroblasts. Endocrinology *134*, 2445–2452.

Zonta, M., Angulo, M.C., Gobbo, S., Rosengarten, B., Hossmann, K.A., Pozzan, T., and Carmignoto, G. (2003). Neuron-to-astrocyte signaling is central to the dynamic control of brain microcirculation. Nat. Neurosci. *6*, 43–50.